

# ADEQUACY OF ENGINEERING PREDICTIONS OF SOFT GROUND EFFECT

Keith Attenborough<sup>1</sup>

Timothy van Renterghem<sup>2</sup>

<sup>1</sup> School of Engineering and Innovation, The Open University, MK7 6AA, UK

<sup>2</sup> Department of Information Technology, WAVES research group, Ghent University, 9052 Ghent-Zwijnaarde, Belgium  
keith.attenborough@open.ac.uk

## ABSTRACT

It is commonly the case that the attenuation due to destructive interference between sound reflected from the ground surface and the sound propagating directly between the source and receiver is included in engineering schemes for predicting outdoor sound propagation. The formulae for soft ground effect in CRTN, CRN, ISO9613-2, HARMONOISE (HP2P) and in the scheme intended for use in noise mapping according to the European Noise Directive (CNOSSOS-EU) are outlined. The importance of including ground cover vegetation effects is discussed. Engineering scheme predictions and those of a detailed numerical method (FDTD) are compared with data for propagation from traffic over soft profiled terrain. Predictions of ground effect near wind turbines assuming single and multiple point sources are compared. There is scope for improving the accuracy of engineering schemes for calculating soft ground effect, particularly when assessing the potential for mitigating noise by ‘softened’ ground, vegetation, berms or tree belts.

## 1. INTRODUCTION

CRTN [1] and CRN [2] are source specific schemes for the prediction of road and rail noise levels respectively in urban environments. In CRTN, the correction for the ground effect attenuation,  $\Delta_{GC}$ , is a function of the horizontal distance from edge of nearside carriageway  $d$  ( $d \geq 4$ ), the average height of propagation,  $\bar{h} = 0.5(h + 1)$  m, and the proportion of absorbent ground,  $I$ ,

$$\begin{aligned} \Delta_{GC} &= 5.2I \log_{10} \left( \frac{6\bar{h}-1.5}{d+3.5} \right) & \text{if } 0.75 \leq \bar{h} < \frac{d+5}{6} \\ \Delta_{GC} &= 5.2I \log_{10} \left( \frac{3}{d+3.5} \right) & \text{if } \bar{h} < 0.75 \\ \Delta_{GC} &= 0 & \text{if } \bar{h} \geq \frac{d+5}{6} \end{aligned} \quad (1)$$

Equivalent expressions in CRN are

$$\begin{aligned} \Delta_{GC} &= -31 \log_{10}(d/25) & \bar{h} \leq 1 \\ \Delta_{GC} &= -0.61(6 - \bar{h}) \log_{10}(d/25) & 1 \leq \bar{h} \leq 6, \\ \Delta_{GC} &= 0 & 6 < \bar{h}. \end{aligned} \quad (2)$$

where  $d$  is the horizontal distance between near side rail and the reception point and  $\bar{h}$  is the mean height of the propagation path. In ISO 9613-2 [3], any low porosity surface is considered acoustically hard and any grass-, tree-, or vegetation- covered ground is considered acoustically soft.

ISO 9613-2 specifies a source region occupying a distance  $30h_s < d_p$  from the source towards the receiver, a receiver region occupying a distance  $30h_r < d_p$  from the receiver towards the source and a middle region occupying the distance

between the source and receiver regions. If  $d_p < (30h_r + 30h_s)$ , there is no middle region. The acoustic properties of each ground region are specified by a ground factor,  $G$ , which is 0 for hard ground (paving, water, ice, concrete and other surfaces with low porosity), 1 for grassland, trees, vegetation, farmland and between 0 and 1 for a mixture of hard and porous ground.

The combined ground effect is calculated from

$$A_{ground} = A_s + A_r + A_m \quad (3)$$

where  $A_s$ ,  $A_r$  and  $A_m$  are the source, receiver and middle region components of the attenuation with corresponding ground factors  $G_s$ ,  $G_r$  and  $G_m$ . When much of the ground is porous and the sound is not a pure tone, the ground attenuation (dB) can be calculated by the formula

$$A_{ground} = 4.8 - (2h_m/d)(17 + 300/d) \quad (4)$$

Like the ISO scheme, the CONCAWE scheme [4] is essentially empirical and was derived for use by the petrochemical industry. As in the ISO scheme, CONCAWE allows for there being both acoustically hard and acoustically soft ground along the propagation paths. However, only the distance travelled over the soft ground is used for calculating the ground effect correction which is in octave bands. Moreover, rather than being confined, to ‘moderate downwind’ as in the ISO scheme, predictions can be made for a wide range of meteorological conditions.

The HARMONOISE project [5] developed source-independent schemes for outdoor sound prediction. As in NORD2000 [6], state-of-the-art numerical reference models were used to validate a simpler engineering model. The engineering version (HP2P) calculates in one third octave bands or octave bands for each sound source and combines these predictions into the day-night equivalent continuous level,  $L_{den}$ .

The contribution of the ground reflection, relative to free field sound propagation, is

$$\Delta L_G = 10 \log_{10} \left( \left| 1 + C_{coh} Q \frac{R_d}{R_g} e^{jk(R_g - R_d)} \right|^2 + (1 - C_{coh}^2) \left| Q \frac{R_d}{R_g} e^{jk(R_g - R_d)} \right|^2 \right) \quad (5)$$

where  $R_d$  is the direct path length between source and receiver,  $R_g$  is the ground reflected path length,  $k$  is the wave number,  $Q$  is the spherical ground reflection coefficient and the coherence factor  $C_{coh}$  is 1 if the direct and ground-reflected arrivals are completely coherent and 0 if they are totally incoherent.

The HP2P model accounts for impedance discontinuities by means of a Fresnel zone method, i.e.

$$\Delta L_{G,mixed} = \sum_{i=1}^{N_m} w_i \Delta L_{G,i} \quad (6)$$

where  $w_i$  is the Fresnel weight of ground in zone  $i$ ,  $N_m$  is the number of different ground types encountered in between source and receiver, and  $\Delta L_{G,i}$  is the partial ground reflection contribution for (flat, uniform) ground type  $i$  between source and receiver.

The method to be used for strategic noise mapping under the Environmental Noise Directive (2002) (END/CNOSSOS) [7] is similar to ISO9613-2 [3] in that it allows for frequency-dependent ground effect over non-flat ground by defining equivalent heights and uses a dimensionless frequency independent coefficient, ground factor,  $G$ , with values between 0 (acoustically hard) and 1 (acoustically soft) according to the type of ground. Likewise, the END scheme introduces a factor,  $G_{path}$ , the fraction of the path occupied by porous ground, corrected if the receiver is sufficiently close to the source.

$$G'_{path} = G_{path} \left[ \frac{d_p}{30(z_S + z_R)} \right] + G_S \left[ 1 - \frac{d_p}{30(z_S + z_R)} \right], \text{ if } d_p \leq 30(z_S + z_R) \\ = G_{path} \quad \text{else,} \quad (7)$$

where  $d_p$  is the source to receiver distance,  $z_S$ ,  $z_R$  are the source and receiver heights above the mean plane between source and receiver,  $G_S$  is the ground factor near the source i.e. 0 for road surfaces and railways on slab tracks and 1 for railways on ballast. As in HARMONOISE and NORD2000, the END scheme lists ground factor values corresponding to eight effective flow resistivity values, based on the single parameter Delany and Bazley model [8], but these are associated with only four values of the  $G$  factor.

The frequency-dependent attenuation due to ground effect under homogeneous atmospheric conditions (no refraction) and without any impedance discontinuities or diffracting edges is given by

$$A_{ground,H} = \max \left[ -10 \log \left( 4 \frac{k^2}{d_p^2} \left\{ z_S^2 - \sqrt{\frac{2C_f}{k} z_S + \frac{C_f}{k}} \right\} \left\{ z_R^2 - \sqrt{\frac{2C_f}{k} z_R + \frac{C_f}{k}} \right\} \right) \right], A_{ground,H,min} \quad (8)$$

$$\text{where } C_f = \frac{1+3wd_p e^{-\sqrt{wd_p}}}{1+wd_p},$$

$$w = 0.0185 \frac{f_m^{2.5} G'_{path}{}^{2.6}}{f_m^{1.5} G'_{path}{}^{2.6} + 1300 f_m^{0.75} G'_{path}{}^{1.3} + 1160 \times 10^3},$$

$$A_{ground,H,min} = -3(1 - G'_{path}),$$

$k = 2\pi f_m / c$ , and  $f_m$  Hz is the centre frequency of the frequency band considered.

## 2. SOFT GROUND EFFECT COMPARISONS

The distance correction in CRTN is  $\Delta_d = -10 \log_{10}(d_s/13.5)$  ( $d_s \geq 4$  m), and in CRN it is  $\Delta_d = -10 \log_{10}(d_s/25)$  ( $d_s \geq 10$  m), where  $d_s$  is the slant distance from source to reception point. Figure 1 shows predictions of attenuation rates with (horizontal) distance between source and receiver at 1.2 m height, due to ground effect and air absorption alone (i.e. excluding wave front spreading which is different for the different sources) with reference to the values at 25 m (this is the reference distance for CRN). The CRTN and CRN curves have been calculated assuming source heights of 0.5 m and 0 m respectively and give roughly comparable results. The air absorption term,  $(0.002d + 0.2)$ , causes the linear behaviour of the CRN predictions at longer ranges. The ISO prediction

curves are based on use of eqn. (4) and the air absorption value for 500 Hz assuming 20°C and 70 % RH ( $\alpha = 2.8$  dB/km). Note that the ISO scheme predicts rather lower attenuation rates than the other two schemes beyond 50 m.

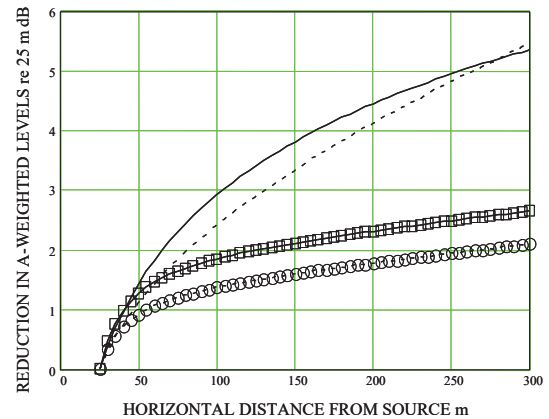


**Figure 1.** Attenuation v distance (re level at 25 m) of A-weighted levels due to soft ground effect and air absorption predicted by CRTN (solid line), CRN (broken line) and ISO 9613-2 for broadband sources at 0.5 m (joined squares) and 0 m height (joined circles).

In the END scheme,  $z_S$  and  $z_R$  (see eqn. (8)) are modified to account for refracted ray paths and turbulence.

$$z'_S = z_S + \delta z_S + \delta z_T \\ z'_R = z_R + \delta z_R + \delta z_T \\ \delta z_S = a_0 \left( \frac{z_S}{z_S + z_R} \right) \frac{d_p^2}{2} \\ \delta z_R = a_0 \left( \frac{z_R}{z_S + z_R} \right) \frac{d_p^2}{2} \\ \delta z_T = 6 \times 10^{-3} \left( \frac{d_p}{z_S + z_R} \right) \quad (9)$$

where  $a_0 = 2 \times 10^{-4}$  is the inverse radius of curvature of the assumed circular downward refracted ray paths.

Figure 2 shows predictions of the attenuation spectra due to soft ground effect with source height 0.5 m, receiver height 4 m and separation of 200 m.

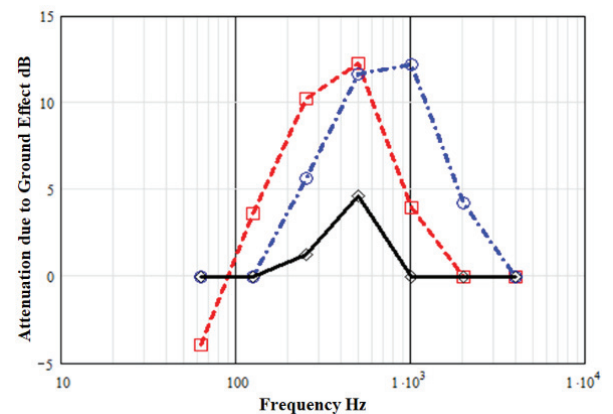


**Figure 2.** Spectra of attenuation due to soft ground effect, with source height 0.5 m, receiver height 4 m and 200 m separation, predicted by ISO9613-2 (squares joined by broken line), the END scheme for an acoustically-neutral atmospheric condition (circles joined by dot dash line) and the END scheme for downwind condition (diamonds joined by continuous line).

The maximum in the spectrum of the attenuation over 'soft' ground predicted by the END scheme for acoustically neutral

conditions is similar in magnitude to that predicted by ISO9613-2 for the same geometry under ‘moderate’ downwind conditions but has an octave higher maximum. This is consistent with the expected difference between the destructive interference due to soft ground effect in acoustically neutral and downward refracting conditions. However, the soft ground attenuation spectrum predicted by the END scheme for downwind conditions (using eqn. (9)) is substantially less than that predicted by ISO9613-2.

Differences such as are shown in Fig. 2 are explored in more detail elsewhere [9]. Also, it should be noted that a consequence of eqn. (7) is that source and receiver are not interchangeable, as required by reciprocity [9].

### 3. SOFT GROUND WITH VEGETATION

As mentioned earlier, while it includes an allowance for foliage on tall vegetation, ISO 9613-2 [3] does not distinguish between grass- or vegetation- covered ground. Moreover, the CRTN, CRN, CONCAWE and END(CNOSSOS) schemes do not allow any extra attenuation due to vegetation cover. Impedance tube and free field measurements have shown that the presence of vegetation increases both the normal incidence and diffuse field absorption coefficient of soils [10,11]. Measurements and predictions have shown that sound propagation through crops is affected by multiple scattering by stems and visco-thermal dissipation in foliage in addition to soft ground effect and, moreover, that growing crops makes ‘soft’ ground ‘softer’ [12]. Through similar mechanisms, hedges have been found also to contribute some extra attenuation [13]. To avoid having to account for all physical mechanisms in detail, it is possible just to add ‘soft’ ground and ‘foliage’ effects, with the latter being calculated from a formula such as [14]

$$\frac{EA(dB)}{\sqrt{FL}} = \frac{\sqrt{ka}}{\left(\frac{0.146}{\sqrt{ka}} + 0.76\right)} \quad (9)$$

where EA represents excess attenuation,  $k = 2\pi f/c$ ,  $F$  is foliage area per unit volume,  $a$  is a mean ‘effective’ foliage dimension and  $L$  is the path length through the foliage.

Calculations have been made for sound propagation to a receiver 50 m from the edge of a two-lane urban road (see Fig.3) and the effect of replacing 47.5 m of hard ground by soft ground on which there are 1 m high crops [12].

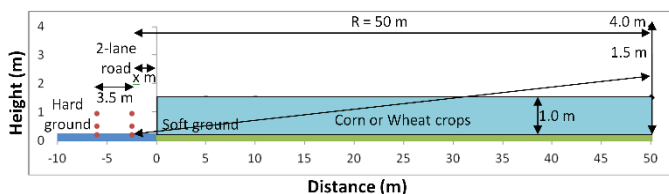


**Figure 3.** The assumed configuration of sources on a two-lane urban road and receivers at either 1.5 m or 4 m height 50 m from the road edge with intervening soft ground and crops.

This configuration involves a single hard-soft impedance discontinuity at 2.5 m and receivers at a horizontal distance of 50 m from the nearest traffic. Each lane is assumed 3.5 m wide with 3.5 m between the two lanes. The source heights are 0.01 m, 0.3 m and 0.75 m depending of vehicle type. It is assumed that the traffic consists of 95 % light vehicles and 5 % heavy

vehicles. The average speed of the vehicles is assumed to be 50 km/h. Compared with propagation over continuous hard ground, extra attenuations are predicted of nearly 15 dB at a 1.5 m high receiver, of which soft ground alone accounts for nearly 9 dB, and 8 dB at a 4 m high receiver, of which soft ground alone accounts for 3 dB. These predictions should be compared with CRTN predictions of 5 dB and 3 dB respectively.

### 4. SOFT BERM NEAR A COMPLEX ROAD

Predictions obtained using three engineering models viz. ISO9613-2, END (CNOSSOS) and HARMONOISE (HP2P) and a Finite Difference Time Domain (FDTD) numerical method have been compared with differences in levels measured at two closely spaced microphones situated near a busy multi-lane road as shown in Fig. 4 [15]. Microphone MP1 was located next to the road at the foot of the rough grass-covered slope of a 6.3 m high berm. Microphone MP2 was situated 80 m from the road in trees at the top of the berm (MP2). Although the trees were sparsely planted, there was a leaf litter layer beneath them.

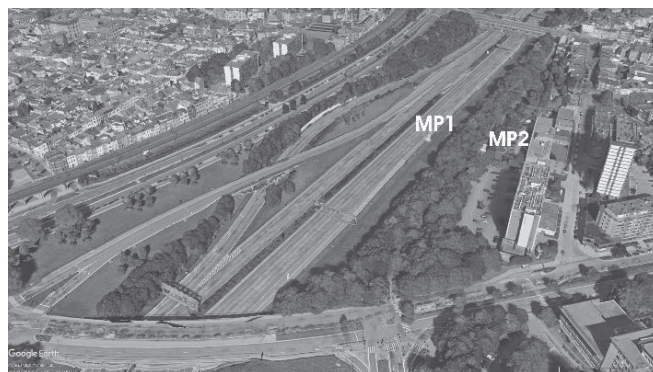


**Figure 4.** Road configuration [15], showing microphone positions MP1 and MP2.

During the one-month noise monitoring period, highly detailed traffic data was available. Also, there was access to digital terrain elevation data with a fine spatial resolution. Measurements were analyzed and predictions made separately for daytime and nighttime since these periods involved different traffic conditions and air absorption. Data obtained during periods with wind speeds above 5 m/s at a reference height of 10 m, according to data from a nearby meteorological observation station, were removed to exclude periods with excessive wind-induced microphone noise. Given that the comparisons involve level differences and short propagation distances, refraction and turbulence effects were ignored in the predictions.

The berm slopes were approximated differently in the various models [15]. For FDTD calculations, the profile was represented by a ‘staircase’ at a very fine spatial resolution of 0.02 m. For HP2P calculations the slope is modelled as a sequence of best fitted linear segments. ISO9613-2 and END (CNOSSOS) prescribe a “median plane” approach, i.e. a best fit on the actual ground profile using a single segment between source and receiver. The latter leads to “effective” source and receiver heights relative to that median plane. For consistency,

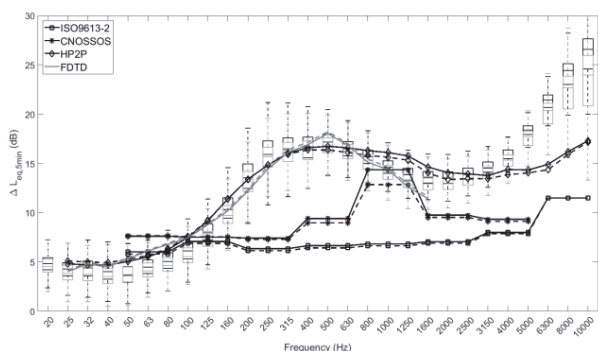
the same source power model values in 1/3 octave bands were used in the predictions.

Table 1 lists parameters used to characterize the surfaces viz. G values for ISO9613-2 and END, (effective) flow resistivity for HP2P, flow resistivity and porosity for FDTD making use of a phenomenological impedance model that has found to enable reasonable fits to short range level difference measurements [8]. For HP2P and FDTD the parameter values are chosen that yield best-fits to the data.

	ISO9613 /END (CNOSSOS)	HP2P	FDTD
surface	G value	n/a	n/a
road	0	rigid	rigid
Berm slope	1	200 kPa s m <sup>-2</sup>	300 kPa s m <sup>-2</sup> , 0.75
leaf litter	1	30 kPa s m <sup>-2</sup>	20 kPa s m <sup>-2</sup> , 0.5

**Table 1.** Parameters used for characterizing the acoustical properties of the surfaces (see Fig. 4) [8, 15].

Figure 5 shows spectra of the level differences recorded between MP1 and MP2. The boxplots indicate the range of measurements (gray boxes are for daytime measurements, black boxes for nighttime measurements). The predictions of the three engineering methods and the reference model are plotted as lines joining the symbols identified in the key. Broken lines represent nighttime predictions and continuous lines daytime predictions.



**Figure 5.** Measured boxplots and predictions of level difference spectra [15].

The ISO9613-2 predictions of sound pressure level difference spectra fail to capture the soft ground effect which is significant between 125 Hz and 1 kHz. Moreover, the ISO9613-2 method significantly underpredicts the measured transmission loss. Possibly, since it allows for different flow resistivity classes and the values used in the predictions were tuned for best fit, the END (CNOSSOS) method seems to give better predictions of the ground effect, but like the ISO9613-2 scheme it underpredicts the transmission loss by several dB. On average, the measured reduction in traffic noise levels between MP1 and MP2 due to the soft berm is about 14 dBA, whereas ISO9613-2 and END (CNOSSOS) predict 7 dBA and 10 dBA, respectively. If either of these models were used to assess different noise abatement solutions for a road configuration

such as shown in Fig. 4, the acoustical effectiveness of a berm would have been underestimated and thereby discounted.

The HP2P model accounts for terrain diffraction, so enables more accurate modelling of the slope's soft ground effect. The resulting predictions are in much better agreement with the measured level difference spectra. While the HP2P scheme is not able to predict the difference in levels between daytime and nighttime, this is less than 1 dBA in most 1/3 octave bands.

To reduce the computational cost the maximum frequency of FDTD prediction was limited to the upper frequency of the 1/3 octave band with centre frequency 1.6 kHz. Nevertheless, the FDTD method yields predictions in close agreement with both the measured level difference spectra and also the total A-weighted sound pressure level difference (<0.5 dBA) [15]. Moreover, the FDTD simulations predict the observed differences between day and night transmission losses. The ability to predict such effects, although small, shows the accuracy and high sensitivity of the FDTD method and the importance of including the details of such a complex example when making predictions.

Additional analysis using FDTD [15] has shown the importance of the different soft ground attenuation associated with the leaf litter near the top of the berm. If the embankment is assumed to be completely grass-covered, the level difference is predicted to be about 3 dBA lower. This suggests that, in situations such as in this example, accurate predictions require detailed soft ground modelling. On the other hand, calculation times with FDTD are a few orders of magnitude larger than when using the engineering methods.

## 5. SOFT GROUND EFFECT NEAR WIND TURBINES

In many detailed outdoor sound propagation models and engineering models, wind turbine sound emission is represented by an 'effective' point source placed at hub height [16]. The source power spectrum is estimated by calculating back from a sound pressure level spectrum measured close to this virtual hub height position. In this way, the energy from the noise sources distributed all over the wind turbine rotor plane is assumed to be concentrated at the effective point source position. An alternative is to model sound propagation from a wind turbine as though it is from a series of (incoherent) noise sources in the rotor plane, positioned at the blade tips or very close to it. Simple analytical considerations in a non-refracting homogeneous atmosphere have indicated that the difference in sound pressure levels due to a single hub source and distributed tip noise sources is less than 1 dB at a distance exceeding the rotor diameter [17].

Here a comparison is made between the results of predictions using ISO9613-2 and HP2P that assume that the source power is concentrated at hub height or, using HP2P, that the same total acoustic energy is distributed over 100 blade tip positions (see Fig. 6) such that the energy contributed by each source is added at the receiver. Refraction by the atmosphere is neglected but this is justifiable for short propagation distances in combination with a highly elevated source.

The average spectrum for large horizontal axis wind turbines (> 2MW), as reported in [18] based on a large dataset of measurements, was used.

The ground near the wind turbine is assumed to be “grassland”.

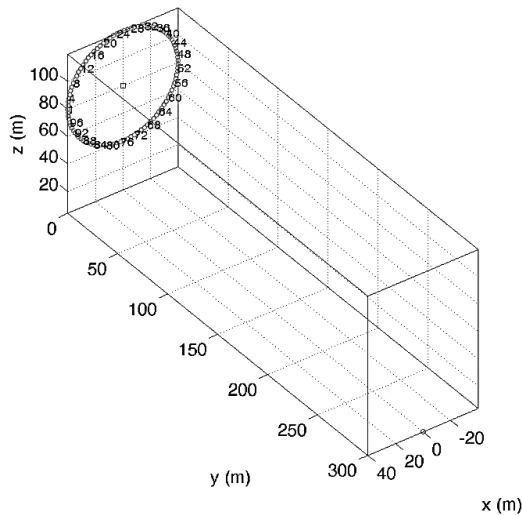


**Figure 6.** Geometry used in the example calculations of wind turbine sound propagation with engineering methods. The numbers indicate the blade tip point source positions in the rotor plane.

Predictions spectra at a 4 m high receiver 300 m from the turbine rotor plane are shown in Fig. 7 (octave bands for ISO9613-2 and 1/3 octave bands for HP2P). The assumption of a single point source modelling leads to pronounced spectral dips in fractional octave bands which disappear when integrating the contributions from multiple source points

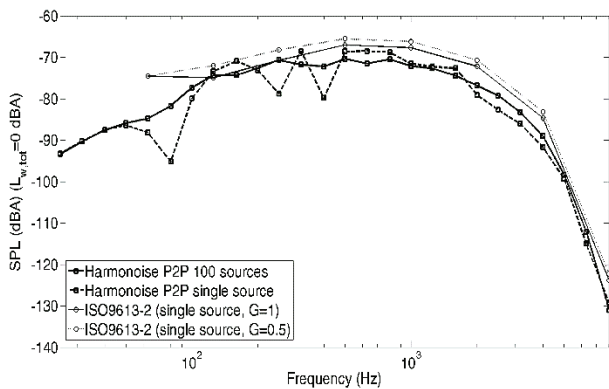


**Figure 7.** Sound pressure level spectra predicted using ISO9613-2 (octave band) and HP2P (1/3 octave band) for a single effective source and using HP2P for distributed sources (see Fig. 6).

Using HP2P with distributed sources results in a total sound pressure level prediction that is 0.7 dBA lower than that obtained by concentrating the sound energy at hub height. ISO9613-2 with a single effective point source and  $G = 1$  predicts a level that is 2.2 dBA lower. Also shown is the result of using the ISO9613-2 scheme with  $G = 0.5$  as has been suggested [19]. This leads to a difference in predictions of only 0.5 dBA between ISO9613-2 and HP2P when assuming a single effective source.

## 6. CONCLUDING REMARKS

Although the use of detailed numerical modelling for predicting outdoor sound propagation remains impractical for engineering purposes, some drawbacks of engineering models have been highlighted. Specifically, attenuation rates due to soft ground effect predicted by ISO9613-2 are less than those predicted by engineering models such as CRTN and CRN. While the distinction between classes of ‘soft’ ground in END (CNOSSOS) is to be welcomed, and an empirical correction to ISO9613-2 may improve its usefulness for predicting soft ground effect near wind turbines, both END (CNOSSOS) and ISO9613-2 have been shown to significantly underestimate the effect of a soft berm next to a highway. Accuracy could be improved by accounting for the presence of vegetation as well as soft ground. The engineering scheme HP2P developed by the European HARMONOISE and IMAGINE projects is more sophisticated, but methods such as ISO9613-2 and END (CNOSSOS) are more likely to be used. The systematic underestimation of soft ground effect according to engineering schemes means that, even after allowing for the many sources of uncertainty in predicting outdoor sound propagation, use of a berm or the deliberate ‘softening’ of ground, for example by adding vegetation, or as advocated elsewhere [20], may be discounted as potential noise mitigation measures. Particularly in situations where barriers are inappropriate or impractical, the deliberate introduction of soft ground or berms could prove useful.

## 7. REFERENCES

- [1] Calculation of Road Traffic Noise, Department of Transport and Welsh Office, HMSO, 1988.
- [2] Calculation of Railway Noise, Department of Transport, HMSO, 1995.
- [3] ISO9613-2 Acoustics - Attenuation of sound during propagation outdoors - Part 2: A general method of calculation, 1996.
- [4] K. J. Marsh, The CONCAWE model for calculating the propagation of noise from open-air industrial plants, *Applied Acoustics* **15** 411-428 (1982).
- [5] R. Nota, D. Barelds, D. van Maercke. Technical Report HAR32TR-040922-DGMR20 Harmonoise WP 3 Engineering method for road traffic and railway noise after validation and fine-tuning.
- [6] J. Kragh and B. Plovsing, Nord2000. Comprehensive Outdoor Sound Propagation Model. Part I-II. DELTA Acoustics & Vibration Report, 1849-1851/00, 2000 (revised 31 December 2001).
- [7] Directive of the European parliament and of the council relating to the assessment and management of noise 2002/EC/49, 25 June 2002.
- [8] K. Attenborough, I. Bashir and S. Taherzadeh, Outdoor ground impedance models, *J. Acoust. Soc. Am.* **129** (5) 2806 – 2819 (2011)

- [9] A. Kok, Refining the CNOSSOS-EU calculation method for environmental noise, Proc. InterNoise 2019, Madrid (2019)
- [10] K. Horoshenkov, A. Khan, H. Benkreira, A. Mandon and R. Rohr, Acoustic performance of vegetation and soil substratum in an urban context, Ch.3 in *Environmental Methods of Surface Transport Noise Reduction*, ed. Nilsson et al CRC Press, Taylor and Francis (2015)
- [11] M. Connelly, M. Hodgson, Experimental investigation of the sound absorption characteristics of vegetated roofs, *Building and Environment* 92 335 – 346 (2015)
- [12] I. Bashir, S. Taherzadeh, H.-C. Shin, K. Attenborough, Sound propagation over soft ground with and without crops and potential for surface transport noise reduction, *J. Acoust. Soc. Am.* 137 154 – 164 (2015)
- [13] T Van Renterghem, K Attenborough, M Maennel, J Defrance, K Horoshenkov, J Kang, I Bashir, S Taherzadeh, B Altreuther, A Khan, Yu Smyrnova, H-S Yang, Measured light vehicle noise reduction by hedges, *Applied Acoustics* 78 19 – 27 (2013)
- [14] K. Attenborough, T. Van Renterghem, *Predicting Outdoor Sound*, 2<sup>nd</sup> edition, Taylor and Francis (in press)
- [15] T. Van Renterghem, D. Botteldooren, Landscaping for road traffic noise abatement: model validation, *Environmental Modelling and Software*, 109, 17 – 31 (2018)
- [16] H. Møller, CS Pedersen, Low-frequency noise from large wind turbines. *J. Acoust. Soc. Am.* 129 3727–3744 (2011)
- [17] K. Heutschi, R. Pieren, M. Müller, M. Manyoky, UW Hayek, K. Eggenschwiler, Auralization of wind turbine noise: propagation filtering and vegetation noise synthesis. *Act. Acust. Acust.* 100, 13 – 24 (2014)
- [18] B. Søndergaard. Low Frequency Noise from Wind Turbines: Do the Danish Regulations Have Any Impact? An Analysis of Noise Measurements. *International Journal of Aeroacoustics* 14 (5-6), 909-915, 2015.
- [19] M. Cand, R. Davis, C. Jordan, M. Hayes, R. Perkins, A good practice guide to the application of ETSU-R-97 for the assessment and rating of wind turbine noise, Institute of Acoustics, 2013
- [20] K. Attenborough, I. Bashir and S. Taherzadeh, Exploiting ground effects for surface transport noise abatement, *Noise Mapping Journal*, 3 1- 25 (2016).